Journal of Materials Processing Technology 246 (2017) 267–275

Contents lists available at ScienceDirect

Journal of Materials Processing Technology

journal homepage: www.elsevier.com/locate/jmatprotec

Ameliorated longitudinal critically refracted—Attenuation velocity method for welding residual stress measurement

Qimeng Zhu [a], Jia Chen [a,b], Guoqing Gou [a,*], Hui Chen [a], Peng Li [c]

[a] School of Materials Science and Engineering, Southwest Jiaotong University, Chengdu 610031, China
[b] Chengdu Industry and Trade College, Chengdu 611731, China
[c] CSR Qingdao Sifang Co. Ltd., Qingdao 266000, China

ARTICLE INFO

Article history:
Received 14 July 2016
Received in revised form 28 February 2017
Accepted 22 March 2017
Available online 24 March 2017

Keywords:
Welding residual stress measurement
Longitudinal critically-refracted (LCR)wave
Wave velocity
Wave attenuation
Microstructure effect

ABSTRACT

This work aims at quantitative analysing the effect of different microstructures on the velocity at stress-free and stress coefficient (K) of longitudinal critical refraction (LCR) wave in measuring welding residual stress process, ameliorating the traditional LCR wave method for improving its' effectiveness and accuracy. The longitudinal critically refracted wave attenuation velocity (LCR-AV) method was proposed in the evaluation of residual stresses in A7N01 welded joints. The same initial status base materials samples are used to produce different levels of grain size and precipitation by heat treatment technology, obtained the velocity at stress-free and attenuation of LCR wave. As expected, the voltage amplitude changes linearly with velocity and stress coefficient, and the precipitation effect can be ignored. The LCR-AV method based on the liner relationship between velocity, attenuation and grain size are efficient to decrease the errors resulting from the different microstructure (base metals, heat-affected zones, and welded zones). Differ with the traditional LCR waves method, the LCR-AV method also measures the voltage amplitude, and the measured results of LCR-AV method compared with those obtained by the hole-drilling reference method shows more sufficient measurement reliability and precision. It shows that LCR-AV method is a valuable quantitative technology to estimate the residual stress of welded joints.

1. Introduction

The detriments of tensile residual stress are investigated by Webster and Ezeilo (2001) where residual stress exiting on surface or subsurface of welded joints will accelerate cracks initiation and growth when they are combined with external cyclic loads applied on the structures. Estimating the residual stress levels and distributions in welded structures are indispensable for quantitative assessing the reliabilities of mechanical equipment and useful for industries. Several methods are accessible for stress measurement including the hole-drilling method, contour methods (Lee and Liu, 2009), X-ray diffraction method (Martins et al., 2006), and neutron diffraction (Sahu et al., 2016).

Within the elastic range, the time of flight(TOF) of the LCR wave presents a good liner relationship with the corresponding uniaxial stress when the propagation acoustic path is fixed. Hughes et al. (1950) proposed a formula for isotropic materials based on acoustoelasticity theory which leads to the following rapid development of ultrasonic stress measurement. Ultrasonic stress measurement is classified into various groups according to different types of waves which could be employed for nondestructive stress measurement on metals including longitudinal wave, transverse wave, and surface wave and others.

A special longitudinal bulk wave mode is utilized in LCR wave stress measurement, as shown in Fig. 1, mainly propagating beneath the surface at a certain depth depended on the frequency of transducers. According to the Snell law(Wennerberg, 2010), when a beam of longitudinal wave with a certain inclination angle reaches to media 2 from media 1. A part enters into the medium 2, and is separated into refracted longitudinal wave and refracted shear wave. In Fig. 1, θ_0 is incidence angle, θ_L is longitudinal wave refraction angle and θ_S is shear wave refraction angle. When longitudinal wave refraction $\theta_L = 90^\circ$, the incidence angle θ_0 is called the first critical angle and refraction longitudinal wave is called longitudinal critically refracted(LCR) wave. Among all the waves, the LCR wave exhibits the largest sensitivity to the same direction stress and highest accuracy of measurement results according to the experiments finished by Egle and Bray (1976). Javadi et al. (2014)

* Corresponding author at: School of Materials Science and Engineering, Southwest Jiaotong University, No. 111, North 1st Section of Second Ring Road, Jinniu District, Chengdu, Sichuan Province, China.
E-mail address: gouguoqing@swjtu.edu.cn (G. Gou).

http://dx.doi.org/10.1016/j.jmatprotec.2017.03.022
0924-0136/

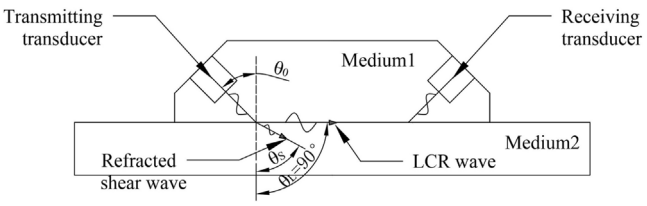

Fig. 1. Schematic diagram of LCR transmission.

combined the ultrasonic stress measurement with finite element method which proved that the resolution of LCR method is suitable enough to distinguish the influence of using the clamp on the longitudinal residual stresses of the stainless steel plates. Javadi et al. (2013a,b,c) also measured the welding residual stresses in dissimilar welded pipes by LCR wave, and pointed out that the obstacles preventing the LCR wave method in measuring dissimilar welding residual stress. Javadi and Mosteshary (2016) validated the enough accuracy of LCR wave method to evaluate the sub-surface residual stresses of the pressure vessel by the finite elements(FE) simulation. Sadeghi et al. (2013) developed FELCR method and confirmed its potential ability to evaluate through-thickness stress of aluminum plates.

However, a number of factors including grain size (Kumaran, 2011 and Alexandre Aparecido Buenos et al., 2014), texture (Ploix et al., 2005), anisotropy (Pereira and Santos, 2013) and grain structure(Nam et al., 2006), can negatively influence the measurement accuracy of ultrasonic stress measurement. Li et al. (2016) studied the application of the LCR wave in monitoring internal residual stress at the service condition and noticed that the grain size was the key factor that affecting the accuracy of LCR wave method. Significantly, Qozam et al. (2006) measured the residual stress of welded joints and took the influences resulted from the different microstructures into consideration, and Qozam et al. (2010) then evaluated the acoustoelastic constant and TOF at a stress-free state directly in the fusion zone of a welded zone in the P460 and P265 steels. According to their researches, the residual stress of traditional LCR wave method was over estimated by 20–30% degree with the ignoring the microstructure effect.

Several research studies have been carried out by employing ultrasonic waves to evaluate the grain size of metals based on the relationships between the attenuation or velocities of ultrasonic waves and the grain sizes. Bouda et al. (2003) presented an experimental setup for ultrasonic grain size measurement by employing ultrasonic wave attenuation and velocity respectively and their research confirmed that the attenuation of an LCR wave can be used to characterize the mean grain size precisely. Sarpün et al. (2005) evaluated the mean grain size of marble by ultrasonic wave where they concluded the relationship between ultrasonic velocity and mean grain size of marble. Buenos et al. (2014) further studied the influences of LCR wave velocity resulted from grain size of low carbon steel and they even developed a numerical model connecting the mean grain size and velocity of the LCR wave for quantitative assessment their mean grain size.

However, there are rare publications investigated the online correcting strategies for eliminating or reducing LCR wave measurement errors in measuring welding residual stress process. In this paper, we measured the attenuation and velocity at stress-free condition of A7N01 alloy samples with different grain size and precipitation, respectively. The quantitative relationships between attenuation, velocity at stress-free condition and stress coefficient K are proposed, while the LCR-AV method is based on these relationships. Fortunately, there is an acceptable agreement between the hole-drilling results and those obtained from the LCR-AV method. The LCR-AV method proposed above is a practical non-destructive evaluation approach for measuring welding residual stress and suitable for industrial application.

2. LCR-AV method

Within the elastic limit, the ultrasonic stress measurement relies on the linear relationship between the stress and the TOF change, i.e. The relationship between TOF measured by the LCR wave and the corresponding uniaxial stress is derived by Egle and Bray (1976). The sensitivity of ultrasonic waves to the strain has been studied in tensile and compressive load tests for rail steel which proved that the sensitivity of LCR waves to the strain is highest (Egle and Bray, 1976). In recent years, ultrasonic stress measurement using piezoelectric transducers have been proposed to detect and identify damage in complex structures (Liao et al., 2015). The piezoelectric transducers are used in this paper for inducing or receiving ultrasonic waves, and getting LCR wave. The schematic diagram of the LCR waves for evaluating the residual stress is described in Fig. 1. The first critical angle can be calculated with the following equation:

$$\theta_{\mathrm{LCR}} = \sin^{-1}(V_1/V_2) \tag{1}$$

where V_1 and V_2 are wave velocity in media 1 and 2, respectively; θ_{LCR} is the first critical angle. As shown in Fig. 1, θs is the shear angle of refraction; θ_L is the longitudinal wave angle of refraction.

The velocity of the longitudinal waves traveling parallel to the load direction related to the strain (α) can be summarized as the following Eq. (2):

$$\rho_0 V_{11}^2 = \lambda + 2\mu + (2l + \lambda)\theta + (4m + 4\lambda + 10\mu)\alpha_1 \tag{2}$$

where V_{11} is the wave velocity of longitudinal wave propagating parallel to load; ρ_0 is the initial density of material without stress; λ, μ are the second order elastic constant (Lame's constant); *l, m, and n* are the third order elastic constants; and α_1, α_2, and α_3 are the components of the homogeneous triaxial principal strains and $\theta = \alpha_1 + \alpha_2 + \alpha_3$. When the stress is in uniaxial status, $\alpha_1 = \varepsilon$, and $\alpha_2 = \alpha_3 = -\mu \times \varepsilon$, where ε is the strain in the direction 1 and υ is the Poisson's ratio. Using those above variables, Eq. (2) becomes:

$$\rho_0 V_{11}^2 = \lambda + \mu + \left[4(\lambda + 2\mu) + 2(\mu + 2m) + \nu\mu\left(1 + \frac{2\lambda}{\mu}\right)\right]\varepsilon \tag{3}$$

The variation of the velocity with the strain representing the relative sensitivity can be calculated by Eq. (4) where L_{11} is the dimensionless acoustoelastic constant for LCR waves.

$$\frac{dV_{11}}{V_{11}ds} = 2 + \frac{(\mu + 2m) + \nu\mu\left(1 + \frac{2l}{\lambda}\right)}{\lambda + 2\mu} = L_{11} \tag{4}$$

Eq. (5) is used to derive the relationship between the stress and LCR wave velocity variations in the corresponding materials:

$$d\sigma = \frac{E dV_{11}}{V_{11}L_{11}} = \frac{E}{L_{11}t_0}dt \tag{5}$$

where $d\sigma$ is the stress variation; E is the elasticity modulus; and dt is the variation of TOF; and t_0 is the time for the wave which travels through a stress-free path in the material being investigated.

From Eq. (5), it can be concluded that E, L_{11}, and t_0 are depended on the nature of materials itself. If k represents E/L_{11}, k can be obtained by using the uniaxial tensile test to characterize the residual stress as shown in Eq. (6).

$$\Delta\sigma = k\frac{t - t_0}{t_0} \tag{6}$$

where t is the ultrasonic wave TOF in test samples. The path L between the ultrasonic transmitting and receiving transducers is usually fixed. It transforms the relationship between stress and

Table 1
Chemical compositions of base material and welding wire.

Materials	Chemical Composition(wt%)									
	Zn	Mg	Cu	Mn	Cr	Ti	Zr	Si	Fe	Al
A7N01	4.60	1.20	0.10	0.15	0.20	–	0.122	0.35	0.100	Bal.
ER5356	≤0.10	4.5–5.5	≤0.10	0.05–0.20	0.05–0.20	0.06–0.2	–	≤0.25	≤0.10	Bal.

Table 2
Mechanical properties of base material and welding wire.

Material	Tensile Strength (MPa)	Yield Strength (MPa)	Elongation (%)
A7N01	365	295	12
ER5356	265	120	26

velocity change into that between stress and TOF change in a fixed acoustic path, L.

By assuming that K represents k/t_0, Eq. (6) can be simplified to Eq. (7) in which K is called the stress coefficient with the unit of *MPa/ns*.

$$\Delta\sigma = K\Delta t \tag{7}$$

The liner relationships between attenuation, velocity, and grain size can be derived by test experiment for LCR wave. The longitudinal critically refracted wave attenuation velocity (LCR-AV) method based on those relationships combines the information from attenuation and velocity of LCR waves, nevertheless the traditional LCR waves method only collects the velocity.

3. Materials and experiment

3.1. Sample description

Tested material is A7N01 plates with the dimensions of 500 × 450 × 8 mm after welding. The plates are in V-groove with a 1-mm blunt edge. The filler material is ER5356 with the diameter of 1.6 mm. The chemical compositions of A7N01 and ER5356 are listed in Table 1. The mechanical properties of A7N01 and ER5356 are shown in Table 2. To remove the oxides for reducing the porosity of the joints, the surfaces of the alloy were chemically cleaned before welding.

3.2. Hybrid fiber laser-MIG welding

An IPG YLS-4000 fiber laser combined with an KEMPPI KempArc–450 pulse welder was used to fabricate welded samples. The parameters of the fiber laser were as follows: 1.07-μm wavelength, 200-μm core diameter, 4-kW maximum output power, and 0-mm defocusing distance. During the welding process, 99.999% pure argon was utilized as shielding gas from the MIG torch with a paraxial gas nozzle. The welding parameters of the A7N01 are shown in Table 3. However, in order to get wider weld width and HAZ width for studying the efficient of LCR-AV method. A big swing, high voltage, fast wire feed speed and slow welding speed are applied in welding the sample.

3.3. Samples preparation

Twelve tensile samples were prepared by heat-treatment process from the base materials to achieve the desired grain size and precipitation levels. The longitudinal directions of all the samples were parallel to the rolling direction to reduce the influences resulted from their texture. The samples were divided into two groups to quantitative study the influencing factors including grain size and precipitation level on ultrasonic stress measurement, respectively. The samples marked as G2 to G8 (G-group) and S1, S2, S3, and S4 (S-group). Sample G1 without any treatment was used as a reference. The heat treatment conditions and dimensions of the samples are shown in Fig. 2. The G-group samples were heated to 420 °C or 470 °C and held for different times to achieve the desired grain size. The S-group samples were heated to a relative lower temperature of 200 °C, and held for different times to achieve the different precipitation levels.

3.4. Attenuation and time of flight of LCR waves

A 25,000 rpm hand grinder was utilized to abolish the reinforcements and surfaces of samples and water cooling technology was simultaneously employed to control the temperature. The cooling water keeps the grinding temperature under 60 °C to prevent the creation of new thermal stresses. The abolished process is also effective to avoid of being affect before getting K and t_0 by the rough surface and thermal stresses. The attenuation of LCR waves in the samples G-group, and S-group are all measured for studying the relationships between the attenuation, grain size and precipitation level. The wide sound fields of the transducers and the very small variation of ultrasonic wave velocity in the range of actual stress are all the major obstacles in measuring TOF accurately. Fortunately, it will be much easier to get a relative t_0 when the base material sample without stress is used as a reference and assumes its t_0 to be zero. The precise and accurate measurement of TOF are the determined factors affecting the measurement reliability and precision. The accuracy of measuring the attenuation of LCR waves is another key factor for the LCR-AV method. The voltage amplitude of LCR waves can be used to replace the attenuation value since it is relatively easy to measure voltage amplitude of the LCR waves with a high accuracy.

The equipment used to achieve the consistency of the LCR waves in the measured process is shown in Fig. 3. The equipment includes: (a) one data-processing computer, (b) one digital oscilloscope with a sampling frequency of 2.5 GHz, (c) one ultrasonic synchronous signal generator, (d) one transmitting transducer and one receiv-

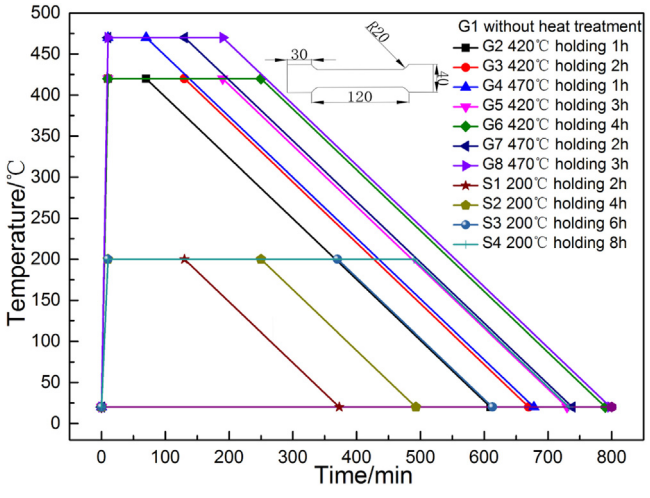

Fig. 2. Heat treatment process diagrams and dimensions for tested samples.

Table 3
Welding process parameters.

Weld	Current (A)	Voltage (V)	Laser Power (kW)	Feeding Speed(m/min)	Welding Speed (m/min)
Filler1	235	21	1	9	10
Filler2	271	27	3	11	10

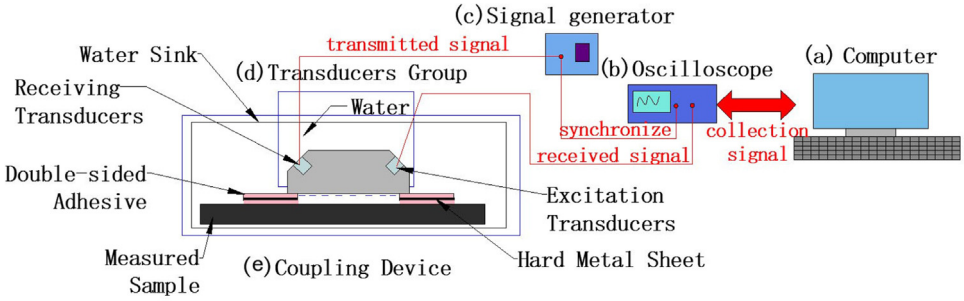

Fig. 3. Sketch of the measured device.

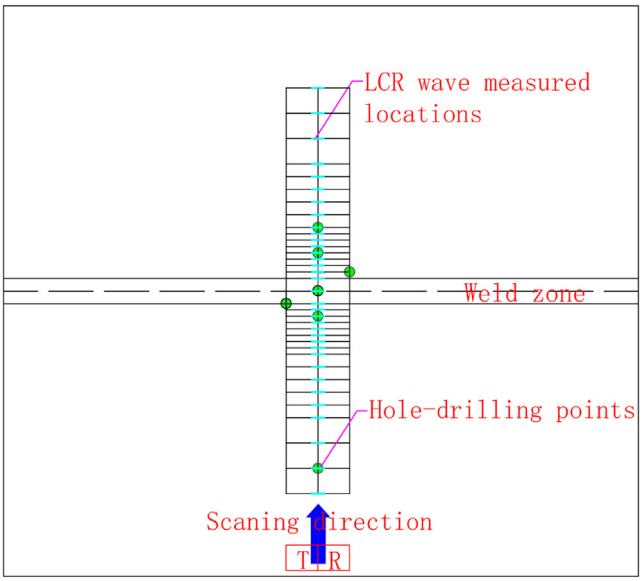

Fig. 4. Sketch of measured points or locations.

ing transducer with frequencies of 2.25 MHz, and (e) one Plexiglas wedge for embedding the transducers and attaching double-sided adhesive and hard-metal sheets. In addition, a temperature sensor was used for measuring the change of temperature that was not marked in Fig. 3.

Keeping consistent coupling state including the couplant film thickness and pressure is essential for measuring the voltage amplitude and TOF of LCR wave. Any change in the couplant film thickness and pressure can lead to a variation of TOF and voltage amplitude, which results in a measurement error. This constant pressure and film thickness, controlled by (e) coupling device as shown in Fig. 3. The double-sided adhesive connects the hard-metal sheets and the Plexiglas wedge. A uniform gap is formed between the measuring device and the measured sample which are immersed into a water sink. The couplant film thickness and pressure are determined as a fixed state when the gap is filled by water.

3.5. Calibration of stress coefficient (K)

The stress coefficient (K) needs to be calibrated for the LCR-AV wave method by uniaxial tensile test. The Plexiglas wedge with the embedded ultrasonic transducers was attached to the center of those calibration samples. The direction of the LCR wave transmission is parallel to the longitudinal direction of the calibration samples. The tensile calibration samples are fixed on the stretching machine DNS300. The steady applied load was about 2000 ± 150 N and kept for 20 min. Using the least squares method, linear relationships between the applied stress and the changes in TOF are fitted, and K are the slopes of those fitting lines.

3.6. Evaluation of K and t_0 for welded joints

The welded zone width in this study is 20 mm which is wide enough for attaching the plexiglas wedge in order to measure the stress coefficient (K) and time of flight (t_0) at a stress-free state. The calibration sample was directly cut from the weld plate and the longitudinal direction was parallel to the weld direction. The device in Fig. 3 was used to measure the K and the t_0 in WZ.

3.7. LCR-AV method used for residual stress measurement in welded joints

The measurement process was repeated in each zone located in the scanning path as shown in Fig. 4, which was perpendicular to the weld line and passing from the weld centerline, while the LCR wave propagates parallel to the welding direction. The ultrasonic measured process was conducted over a varying step size. For zones near and on the weld zone (WZ), a step size of 5 or 10 mm was employed, and it was increased to 20 mm for zones further away from the weld(see Fig. 4). Hole-drilling measurements are conducted in different eight points on measured plate including WZ, BM and HAZ as shown in Fig. 4. The results of hole-drilling and the 2.25 MHz LCR-AV method for A7N01 aluminum alloy are compared.

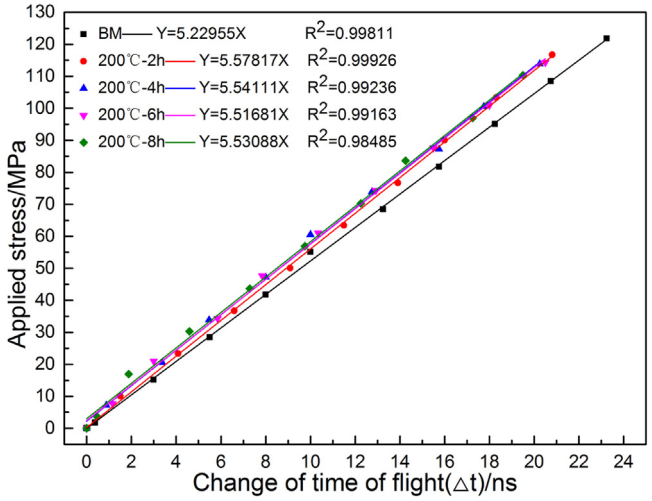

Fig. 5. Results of tensile test to evaluate *K* for the samples with different precipitation levels.

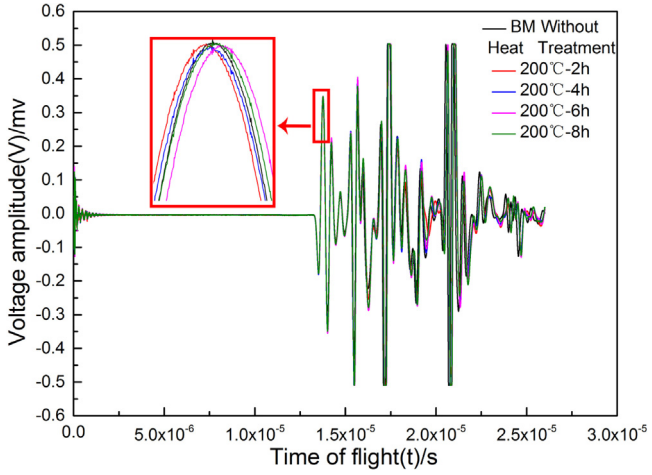

Fig. 6. Voltage amplitude vs. time of flight for the samples with different precipitation levels.

Table 4
Measured t_0 for the samples with different precipitation levels.

Sample	G1	S1	S2	S3	S4
TOF at Stress-free Station (t_0) (ns)	0	−2.0	−0.8	2.0	0.4
Voltage Amplitude (μv)	346.53	346.55	346.04	346.11	346.63
Stress Coefficient (*K*) (MPa·ns-1)	5.23	5.58	5.54	5.52	5.53

4. Results and discussion

4.1. Effect of precipitation levels on K and TOF

The measured TOF vs. the applied stress are plotted and fitted into lines by least square method as shown in Fig. 5. Voltage amplitudes at S1-S4 are measured in Fig. 6. It can be concluded that the *K* and the voltage amplitude are similar between these samples, and the precipitation levels have minor influences on the voltage amplitude and the stress coefficient *K*.

The measured t_0 for the samples with different precipitation levels that are relative to the t_0 of base material (assumed to be zero) have unconspicuous variations as shown in Table 4. The differences of voltage amplitude and stress coefficient between those samples are also small which indicates that the precipitation levels have minor influences on the t_0.

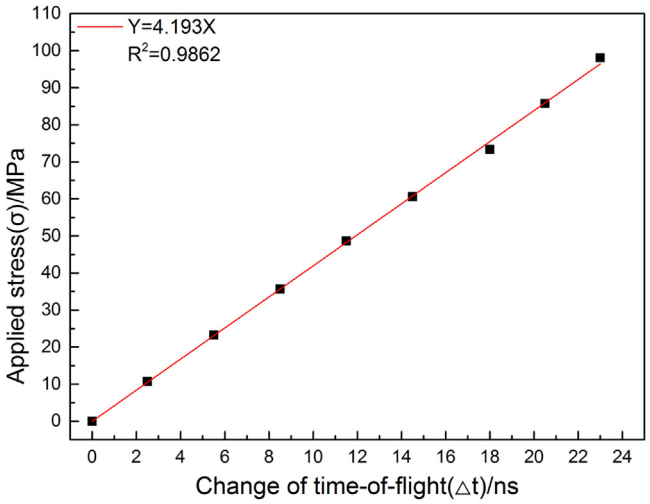

Fig. 7. Result of tensile test to evaluate *K* for weld zone.

The minor effect resulted from precipitation levels on t_0, *K* and voltage amplitude could be attributed to the extremely small geometries of the precipitates being unable to change the state of grain boundaries obviously. Hector Carreon et al. (2016) found that the absorption loss wave predominated in the ultrasonic attenuation of the Ti-6Al–4 V alloy with widmanstatten microstructure(A mesh-like distribution of a precipitating phase in a solid-state transformation which occurs along preferred crystal planes), and widmanstatten grain size are also larger than the other microstructure. The grain boundaries as the main factor affecting the velocity of an ultrasonic wave, the errors in *K*, t_0 and voltage amplitude resulting from precipitation will be relatively small and can be ignored.

4.2. Stress coefficient and time of flight (TOF) in the welded zone

The welding thermal cycles can change the microstructure and mechanical properties of the materials especially the WZ and HAZ. The chemical compositions in the WZ are Al and Mg which are mainly controlled by the filler material ER5356, while the main compositions in HAZ and BM are Al, Zn, and Mg determined by the base materials. It is ineluctable to induce stomatal defects in the WZ, as the researches finished by Wahiba Djerir et al. (2014) that the defects also influence the TOF of LCR wave. Thus, the chemical compositions, microstructure and stomatal defects in WZ are different with that in HAZ and BM attributing to additional influences on the attenuation and velocity of an LCR wave. It is impossible to use the same strategies for eliminating the errors in WZ as that in BM and HAZ, separate measuring the t_0 and *K* for WZ is an efficient method to reduce the error.

Fig. 7 shows the relationship between the applied stress and the change in TOF for WZ. The *K* for WZ can be obtained from the slope of the line which is 4.193, and TOF at the stress-free stage (t_0) is 20.4 ns with the t_0 in BM as a reference (assumed to be zero). If the *K* and t_0 in BM are utilized to evaluate residual stress in WZ without the necessary calibration, the residual stress measured by LCR wave method in WZ will be overestimated.

4.3. Relationship between t_0 and attenuation

Fig. 8 shows the original signals of the measured waves for the G-group samples in which the vertical axis represents the voltage amplitude and the horizontal axis represents the TOF of the ultrasonic wave. To clearly observe the relationship between the TOF and the attenuation, a local amplifying view at the first peak is

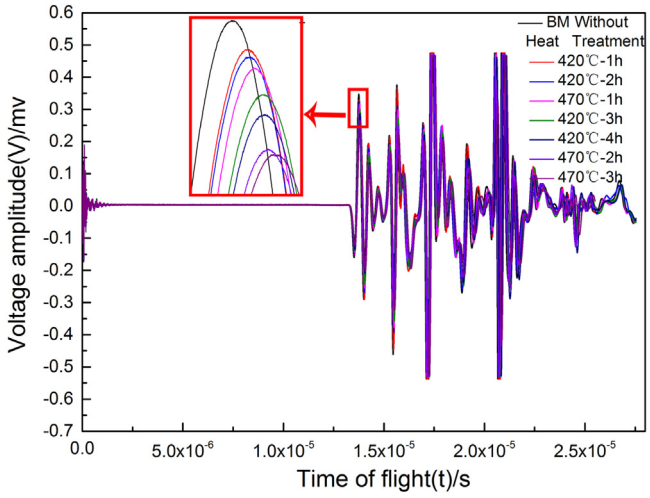

Fig. 8. Original signals of the samples for different grain size.

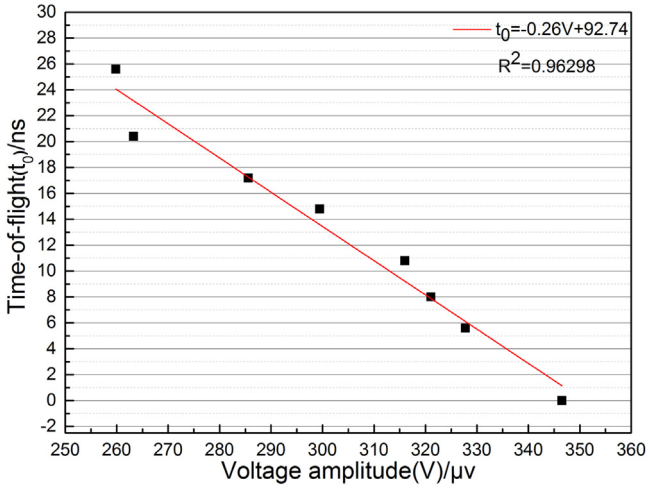

Fig. 9. TOF as a function of voltage amplitude with different grain sizes.

plotted and shown in Fig. 8. From the local view of Fig. 8, the longer holding time is kept, the lower voltage amplitudes and the longer t_0 of LCR wave are measured at the same heat treatment temperature. When the holding time is constant, it can be found that the higher temperature also attributes to the lower voltage amplitudes and the longer t_0 of LCR wave. While not only the longer holding time with some temperature but also the higher temperature with same keeping time are beneficial for getting larger grain.

Table 5 shows the voltage amplitude and t_0 for every sample with different grain size at the stress-free state. It can be found that the t_0 increases and the voltage amplitude decreases as the grain size increases, the increase of t_0 corresponds with decreasing voltage amplitude similarity. These results are consistent with the findings in Refs. Buenos et al. (2014) and Buenos et al. (2012), but the fitted relationship between change in attenuation of LCR wave and grain size is quadratic curve in their researches differing with the almost liner relationship in this research. The data in Table 5 is plotted in Fig. 9 and fitted into the following equation:

$$t_0 = -0.26V + 92.74 \tag{8}$$

where t_0 is the TOF at a stress-free station and V is the value of voltage amplitude.

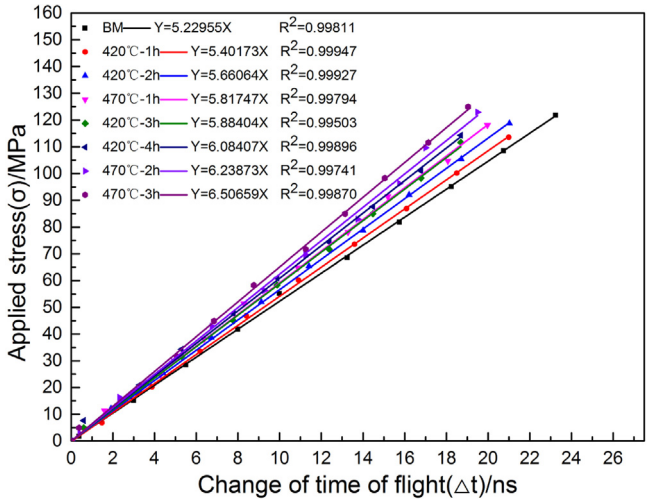

Fig. 10. Results of tensile test to evaluate K for the samples with different grain size levels.

Table 6
Stress coefficient (K) and TOF for samples with different grains size.

Samples	G1	G2	G3	G4	G5	G6	G7	G8
K/MPa ns^{-1}	5.23	5.40	5.66	5.82	5.88	6.08	6.24	6.51

4.4. Relationship between K and attenuation

Fig. 10 shows the fitted relationship between the applied stress and the change of TOF for all G group samples, the slopes of those fitted lines are K listed in Table 6 of those samples according to Eq. (7).

Fig. 11 shows a linear relationship between the K and the V. Voltage amplitude (V) as a function of the stress coefficient (K) is determined by Eq. (9):

$$K = -0.01331\,\mathrm{V} + 9.8 \tag{9}$$

The stress coefficient (K) decreases with increasing of the voltage amplitude. Since fine grain has a lower K according to Table 6, the fine grain will have larger voltage amplitude.

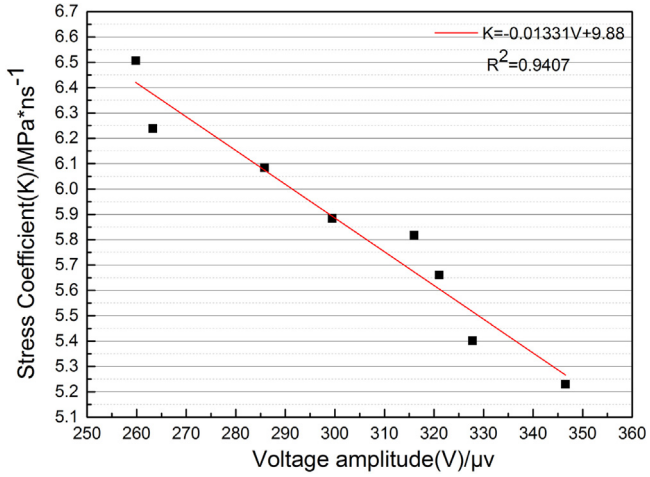

Fig. 11. Stress coefficient as a function of voltage amplitude for samples with different grain sizes.

Table 5
Voltage amplitude and t_0 for samples with different grain sizes.

Samples	G1	G2	G3	G4	G5	G6	G7	G8
V (μv)	346.53	327.78	321.04	316.01	299.47	285.58	263.29	259.81
TOF(ns)	0	5.6	8.0	10.8	14.8	17.2	20.4	25.6

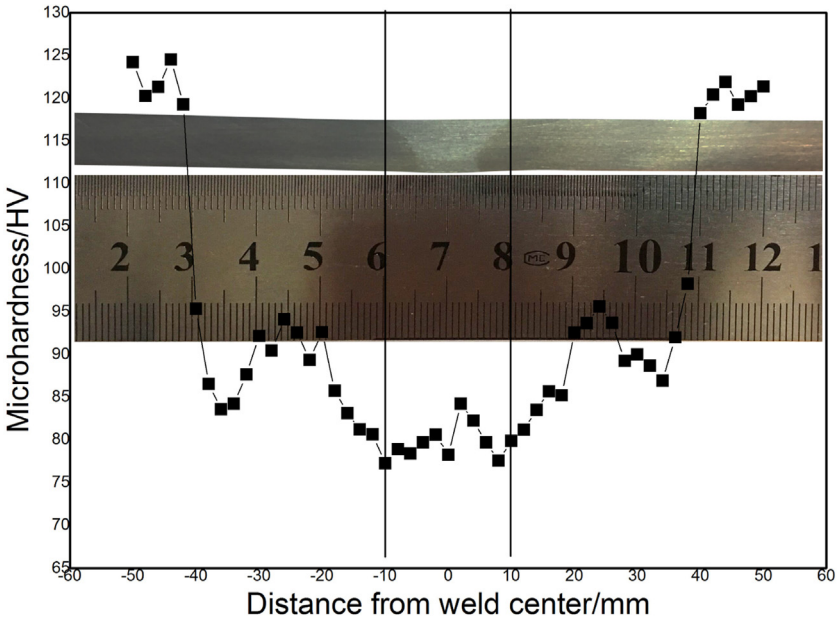

Fig. 12. Hardness and macro of the measured plate.

4.5. LCR-AV method

The relationships between grain size, K, t_0, and attenuation have been established in the above sections, respectively. The welded plate as involved in 3.7 is used to verify the LCR-AV method. It is difficult to observe the HAZ zone by mixed acid, so a hardness test was performed and the results are as show in Fig. 12.

By substituting Eqs. (8) and (9) into Eq. (7), the model formula of LCR-AV method can be obtained as shown in Eq. (10):

$$\Delta\sigma = (-0.01331V + 9.87)[t - (-264.44V + 92.78)] \quad (10)$$

where the measured voltage amplitude (V) and TOF (t) for the welded joints based on the conditions discussed in Section 3.1 can be found in Figs. 13 and 14, obtained with the similar method as discussed in Sections 4.1–4.4, respectively. The change of TOF (Δt) and the voltage amplitudes (V) are almost symmetrical to the weld center as the grain size is the main factor affecting the TOF and the voltage amplitudes, while the grain size is similar at the same distance from the weld center at each side of the weld.

Fig. 14 shows a special phenomenon where the voltage amplitudes at the locations having a distance of 35 mm from the weld center are higher than that in BM. Welding thermal cycles located at this zone equal normalizing inducing fine grain, while finer grain results in higher voltage amplitude based on the above theory and conclusions. In general, the voltage amplitude decreases near the weld because of the coarse grain due to the high temperature during welding.

Fig. 15 shows the distribution of the residual stress measured with hole drilling, traditional LCR and LCR-AV method. The measured results using LCR-AV method are computed with the voltage amplitudes in Fig. 14 and the TOF in Fig. 13, according to Eq. (10). The measured longitudinal residual stresses using the traditional LCR wave method has a significant deviation in the HAZ compared with the hole-drilling method. This is because the grain size in the HAZ is significantly different with that in the BM, which results in the disparity of K and t_0. The largest deviation of the traditional LCR wave method compared to the hole-drilling method is about 107 MPa.While, the largest deviation decreases to about 24 MPa with the LCR-AV method. However, there is a more acceptable agreement between the hole-drilling results and those obtained from the LCR-AV method.

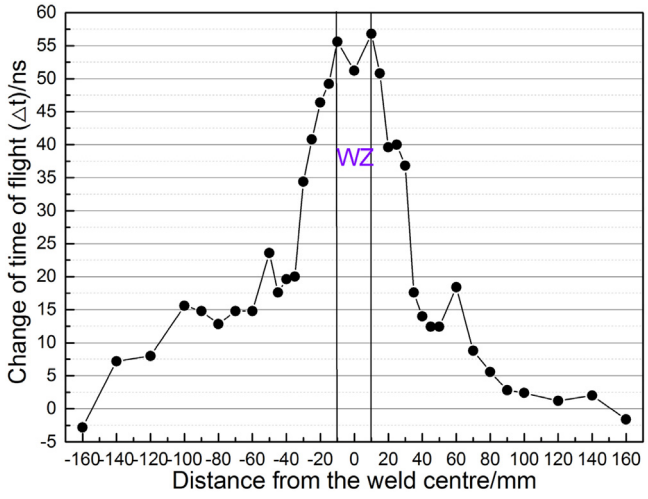

Fig. 13. Time of flight at every measured point.

The measured results using traditional LCR wave method in those locations far away from the weld center are similar to those using LCR-AV method because the microstructure affected in those locations by welding temperature history is small. This comparison shows that the accuracy of LCR-AV method is higher than that of the traditional LCR wave method. To compare the measurement error

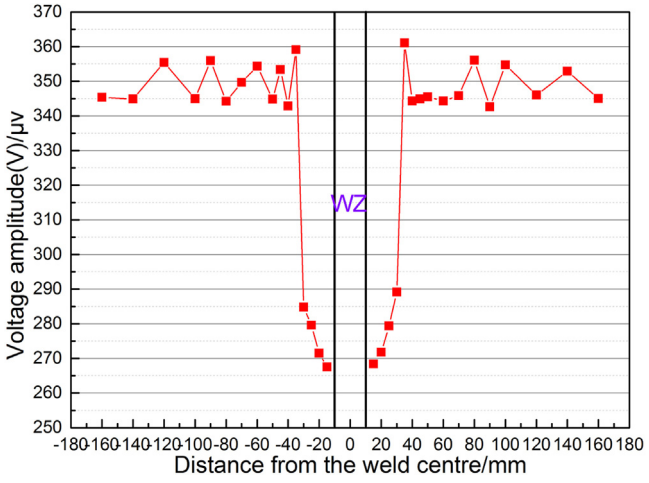

Fig. 14. Voltage amplitude at every measured point.

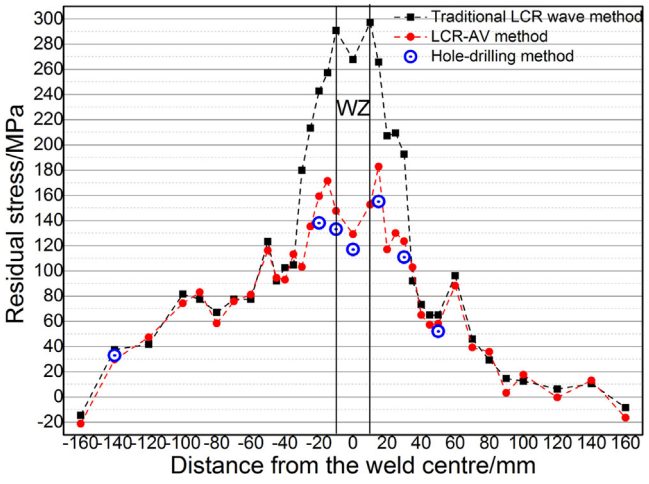

Fig. 15. Measured weld longitudinal residual stress with different methods.

achieved by employing the LCR-AV and hole-drilling method in the field of stress measurement, the following aspects may accountant for the 24 MPa error:

(A) Ignoring the influences resulting from the precipitations and dislocations will attribute to a smaller effect than the grain size, while this paper didn't take the influences into consideration.
(B) The different measured volume between LCR-AV and the hole-drilling method also produces error, the hole-drilling method provided an average stress over the entire 2 mm penetration. The 2.25 MHz LCR-AV measurement penetrated to 2.6 mm based on GB/T 32073-2015. However, the LCR-AV method measures the average of stresses in a determined cuboid, while the hole-drilling method measures the average of stresses in a determined cylinder.

5. Conclusions

The objective of this investigation is to optimize an LCR-AV method to correct the errors resulted from the effects of grain size on the stress coefficient *(K)* and the TOF at stress-free state *(t_0)* in the traditional LCR wave method. Based on the results in this study, the following conclusions could be drawn:

(1) The precipitation level in materials has a minor effect on K and t_0 of LCR waves for A7N01 aluminum alloy, because it is impossible for tiny precipitation to change the large grain boundary shape obviously. This effect can be ignored during stress measurement using LCR-AV method.
(2) The grain size has a significant effect on the K and t_0 of LCR waves. Palpable errors will be observed ignoring the influences due to different grain size levels, largest deviation has been found in HAZ zone for the obvious difference grain size, while the chemical compositions, microstructure and stomatal defects in WZ account for the more obvious effect on the K and t_0 compared with that in HAZ and BM.
(3) Since, both the K and t_0 have a linear relationship with the voltage amplitude, a formula was established for the LCR-AV method based on two variables: V and t_0. The LCR-AV method needs to measure these two variables instead of only t_0 for the traditional LCR wave method in measuring process for evaluating welding residual stress. The LCR-AV method has greatly improved the measurement accuracy compared with the traditional LCR wave method for measuring welding residual stress.

Acknowledgement

The authors acknowledge the financial support from the National Key R&D Program (No. 2015 BAG12B012016YFB1200602-16).

References

Bouda, A.B., Lebaili, S., Benchaala, A., 2003. Grain size influence on ultrasonic velocities and attenuation. NDT E Int. 36, 1–5.
Buenos, A.A., dos Santos, A.A., Pereira, P., Santos, C.S., 2012. Effect of mean grain size in the time of flight for Lcr Waves, ASME International Mechanical Engineering Congress and Exposition. Am. Soc. Mech. Eng., 63–69.
Buenos, A.A., Pereira Jr., P., Mei, P.R., dos Santos, A.A., 2014. Influence of grain size on the propagation of LCR waves in low carbon steel. J. Nondestr. Eval. 33, 562–570.
Carreon, H., Carreon, M., Dueñas, A., 2016. Assessment of precipitates of aged Ti-6Al-4V alloy by ultrasonic attenuation. Philos. Mag., 1–11.
Djerir, W., Ourak, M., Boutkedjirt, T., 2014. Characterization of the critically refracted longitudinal (LCR) waves and their use in defect detection. Res. Nondestr. Eval. 25, 203–217.
Egle, D., Bray, D., 1976. Measurement of acoustoelastic and third-order elastic constants for rail steel. J. Acoust. Soc. Am. 60, 741–744.
Hughes, D., Blankenship, E., Mims, R., 1950. Variation of elastic moduli and wave velocity with pressure and temperature in plastics. J. Appl. Phys. 21, 294–297.
Javadi, Y., Mosteshary, S.H., 2016. Evaluation of sub-surface residual stress by ultrasonic method and finite-element analysis of welding process in a monel pressure vessel. J. Test. Eval. 45.
Javadi, Y., Afzali, O., Raeisi, M.H., Najafabadi, M.A., 2013a. Nondestructive evaluation of welding residual stresses in dissimilar welded pipes. J. Nondestr. Eval. 32, 177–187.
Javadi, Y., Akhlaghi, M., Najafabadi, M.A., 2013b. Using finite element and ultrasonic method to evaluate welding longitudinal residual stress through the thickness in austenitic stainless steel plates. Mater. Des. 45, 628–642.
Javadi, Y., Pirzaman, H.S., Raeisi, M.H., Najafabadi, M.A., 2013c. Ultrasonic inspection of a welded stainless steel pipe to evaluate residual stresses through thickness. Mater. Des. 49, 591–601.
Javadi, Y., Sadeghi, S., Najafabadi, M.A., 2014. Taguchi optimization and ultrasonic measurement of residual stresses in the friction stir welding. Mater. Des. 55, 27–34.
Kumaran, S.M., 2011. Evaluation of precipitation reaction in 2024 Al–Cu alloy through ultrasonic parameters. Mater. Sci. Eng.: A 528, 4152–4158.
Lee, H.-T., Liu, C., 2009. Optimizing the EDM hole-drilling strain gage method for the measurement of residual stress. J. Mater. Process. Technol. 209, 5626–5635.
Li, Z., He, J., Teng, J., Wang, Y., 2016. Internal stress monitoring of in-service structural steel members with ultrasonic method. Materials 9, 223.
Liao, X., Qiu, Z., Jiang, T., Sadiq, M.R., Huang, Z., Demore, C.E., Cochran, S., 2015. Functional piezocrystal characterisation under varying conditions. Materials 8, 8304–8326.
Martins, J.A., Cardoso, L.P., Fraymann, J.A., Button, S.T., 2006. Analyses of residual stresses on stamped valves by X-ray diffraction and finite elements method. J. Mater. Process. Technol. 179, 30–35.
Nam, Y.H., Kim, Y.-I., Nahm, S.H., 2006. Evaluation of fracture appearance transition temperature to forged 3Cr–1Mo–0. 25 V steel using ultrasonic characteristics. Mater. Lett. 60, 3577–3581.
Pereira, P., Santos, A., 2013. Influence of anisotropy generated by rolling on the stress measurement by ultrasound in 7050 T7451 aluminum. Exp. Mech. 53, 415–425.

Ploix, M.-A., GUERJOUMA, R.E., Moysan, J., Corneloup, G., Chassignole, B., 2005. Acoustical characterization of austenitic stainless steel welds for experimental and modeling NDT. J. Adv. Sci. 17, 76–81.
Qozam, H., Hoblos, J., Bourse, G., Robin, C., Walaszek, H., Bouteille, P., Cherfaoui, M., 2006. Ultrasonic stress measurement in welded component by using Lcr waves: analysis of the microstructure effect, materials science forum. Trans. Tech. Publ., 453–458.
Qozam, H., Chaki, S., Bourse, G., Robin, C., Walaszek, H., Bouteille, P., 2010. Microstructure effect on the Lcr elastic wave for welding residual stress measurement. Exp. Mech. 50, 179–185.
Sadeghi, S., Najafabadi, M.A., Javadi, Y., Mohammadisefat, M., 2013. Using ultrasonic waves and finite element method to evaluate through-thickness residual stresses distribution in the friction stir welding of aluminum plates. Mater. Des. 52, 870–880.
Sahu, P.K., Pal, S., Pal, S.K., Jain, R., 2016. Influence of plate position, tool offset and tool rotational speed on mechanical properties and microstructures of dissimilar Al/Cu friction stir welding joints. J. Mater. Process. Technol. 235, 55–67.
Sarpün, İ.H., Kılıçkaya, M.S., Tuncel, S., 2005. Mean grain size determination in marbles by ultrasonic velocity techniques. NDT E Int. 38, 21–25.
Webster, G., Ezeilo, A., 2001. Residual stress distributions and their influence on fatigue lifetimes. Int. J. Fatigue 23, 375–383.
Wennerberg, L., 2010. Snell's law for viscoelastic materials. Geophys. J. R. Astron. Soc. 81, 13–18.